Journal of Molecular Liquids 308 (2020) 113101

Contents lists available at ScienceDirect

Journal of Molecular Liquids

journal homepage: www.elsevier.com/locate/molliq

Extractive detoxification of feedstocks for the production of biofuels using new hydrophobic deep eutectic solvents – Experimental and theoretical studies

Patrycja Makoś *, Edyta Słupek, Jacek Gębicki

Gdansk University of Technology, Faculty of Chemistry, Department of Process Engineering and Chemical Technology, 80 – 233 Gdansk, G. Narutowicza St. 11/12, Poland

ARTICLE INFO

Article history:
Received 30 January 2020
Received in revised form 27 March 2020
Accepted 5 April 2020
Available online 06 April 2020

Keywords:
Hydrophobic deep eutectic solvents
Extraction
Biofuels
Fermentation inhibitors
Detoxification

ABSTRACT

The paper presents a synthesis of novel hydrophobic deep eutectic solvents (DESs) composed of natural components, which were used for removal of furfural (FF) and 5-hydroxymethylfurfural (HMF) from lignocellulosic hydrolysates. The main physicochemical properties of DESs were determined, followed by explanation of the DES formation mechanism, using ^{1}H NMR, ^{13}C NMR and FT-IR analysis and density functional theory (DFT). The most important extraction parameters were optimized. Reusability, regeneration of DES, multistage extraction, influence of FF and HMF concentration, as well as possibility of sugars loss were also investigated. The experimental studies revealed high extraction efficiency resulting in 79.2% and 87.9% removal of FF and HMF respectively from model hydrolysates and in the range of 74.2–76.1% and 87.8–82.3% from real samples in one-step extraction. The yield of bio-hydrogen production via dark fermentation after the DES extraction was comparable to the results obtained using enzymatic hydrolysis. The theoretical studies on the extraction mechanism revealed that hydrogen bonds and van der Waals interactions were the main driving force for detoxification of lignocellulosic biomass.

1. Introduction

For many years lignocellulosic biomass i.e. wood and agricultural residues have been promoted as an attractive resource for the production of biofuels including bioethanol, bio-butanol, bio-methane, and bio-hydrogen [1–4]. The processes of biomass fermentation into biofuels usually require hydrolyzing the carbohydrates into fermentable sugars at first. Currently, acid hydrolysis is one of the major methods for pretreatment of lignocellulosic biomass [5]. However, this method generates fermentation inhibitors such as furfural (FF) and 5-hydroxymethylfurfural (HMF). FF is formed as a dehydration product of pentoses, while HMF is formed from hexoses. They inhibit cell growth, decrease gaseous and liquid biofuels productivity, induce DNA damage and inhibit several enzymes in glycolysis, which contribute to reduced product yield. The amount of fermentation inhibitors depends on the severity of the reaction [6,7]. Theoretically, optimization of the hydrolysis process may result in lower production of toxic compounds. However, lower inhibitors concentration leads to lower sugar yields [8]. To minimize inhibitory effects and increase biofuels yields in the subsequent fermentation step, detoxification of hydrolysates should be introduced.

Up till now, many chemical, physical and biological methods for detoxification of biomass hydrolysate were used, including membrane extraction [9], membrane filtration [10], solvent extraction, adsorption [11], ion-exchange [12], and enzyme adaption of fermenting microorganism [13]. However, most of them are complicated, expensive, require long time operations, create by-products, and could contribute to sugars loss [10]. Among these technologies, liquid-liquid extraction (LLE) is one of the most attractive processes due to its simplicity, economical character, safety, possibility of almost complete removal of fermentation inhibitors from hydrolysates and the ability of easy recovery of FF and HMF from the extraction solvent, what is in line with the biorefinery concept [5]. The type of extraction solvent has a decisive impact on the efficiency of the extraction process. Extraction solvents should be characterized by high affinity towards FF and HMF, low solubility and high stability in aqueous phase, low viscosity, low prices, non-toxicity and should not dissolve sugars. Several common extraction solvents were used i.e. ethyl acetate, isobutyl acetate [14], octanol, isopropyl acetate, toluene [15], o-xylene, m-xylene, and ethylbenzene [16]. Despite the high efficiency of extraction using popular solvents, their recovery in many cases is problematic and requires expensive and an energy intensive solvents recovery unit. In addition, many of the commonly used

* Corresponding author.
E-mail address: patrycja.makos@pg.edu.pl (P. Makoś).

https://doi.org/10.1016/j.molliq.2020.113101

solvents are toxic. Therefore, a lot of research is dedicated to the search for alternative extracting agents.

Recently, a new class of "green solvents", named deep eutectic solvents (DESs), attracts interest due to their physicochemical properties similar to ionic liquids and lower toxicity, cheaper synthesis and higher biodegradability. DESs are the mixtures composed of two or more compounds that are capable of forming eutectic liquids, due to the formation of specific interactions between hydrogen bond donor (HBD) and hydrogen bond acceptor (HBA). Until now, DESs have been successfully used for desulfurization of fuels [17], removal of lignin from biomass [18], sample preparation [19–21], water treatment [22], capture of carbon dioxide [23], biogas purification [24,25], and as electrolyte medium for solar cells [26], etc. However, most of DESs are hydrophilic, which precludes their use as extracting agents for aqueous samples. To date, only a few hydrophobic DESs which selectively dissolve FF and HMF have been developed [15,27].

The paper describes the synthesis of new, never published before hydrophobic DESs composed of ±Camphor (HBA) and 1-decanol, decanoic acid and 3,4-xylenol (HBDs) in 1:2 molar ratio. The characterization of DES was done by ^{1}H NMR, ^{13}C NMR and FT-IR analysis as well as measuring their main physico-chemical properties. In the second part of the studies, DESs were used for removal of FF and HMF from hydrolysates. The extraction process was optimized in terms of parameters selection i.e. kind of DES, time of extraction, temperature, pH, and DES:hydrolysate volume ratio (V_{DES}:V_{HYD}). The reusability and regeneration of DES, multistage extraction, influence of FF and HMF concentration in hydrolysates, as well as possibility of sugars loss were also investigated. For the explanation of the mechanisms of FF and HMF removal, density functional theory (DFT) and FT-IR analysis were applied. Finally, in order to confirm the usefulness of the developed method, purified hydrolysates were subjected to dark fermentation for the production of bio-hydrogen.

2. Experimental

2.1. Materials

The following reagents were used in this study: ±camphor (C), decanoic acid (DecAc), 1-decanol (DOL), 3,4-xylenol (Xyl), 5-Hydroxymethylfurfural, furfural, cellobiose, glucose, xylose, galactose, mannose, arabinose (purity ≥98%), NaOH (purity ≥95%), HCl (purity ≥95%). They were purchased from the Sigma-Aldrich (USA). Compressed gases such as nitrogen (purity N 5,5), air (purity N 5.0) were generated by a DK50 compressor with a membrane dryer (Ekkom, Poland) and hydrogen (purity N 5.5) was generated by a 9400 Hydrogen Generator (Packard, USA).

2.2. Apparatus

Please refer to Supplementary materials – Section S.1.

2.3. Procedures

2.3.1. Preparation of DESs, model and real samples of hydrolysates

Hydrophobic DESs were synthesized by mixing ±camphor as (HBA) and 1-decanol, decanoic acid or 3,4-xylenol (HBD) in the 1:2 molar ratio. The mixtures were heated at 70 °C for 30 min using hot plate stirrer until clear solutions were obtained.

Model hydrolysate was prepared by dissolving cellobiose (5.18 g/L), glucose (10.14 g/L), xylose (5 g/L), galactose (4.76 g/L), mannose (4.85 g/L), arabinose (5.07 g/L), FF (5.2 g/L) and HMF (5.1 g/L) in water.

Freshly chopped (mesh = 0.75 mm) energetic willow (*Salix viminalis* L), with the following composition: cellulose 46.5 ± 0.1%, hemicellulose 15.6 ± 0.08%, lignin 29.4 ± 0.05, ash 0.6 ± 0.01%, moisture 7.0 ± 0.05%, was used for the preparation of real sample of the first hydrolysate (EW NaOH). The hydrolysate was obtained by the alkaline pre-treatment of the energetic willow, which was carried out using 6% NaOH solution. The reaction flasks were incubated in a shaker at 60 °C for 6 h [28]. The second hydrolysate (EW MEA) was prepared via the alkaline pre-treatment, with 21% monoethanolamine, of the energetic poplar *Populisindustria* (mesh = 0.75 mm), with the following composition: cellulose 39.5 ± 0.1%, hemicellulose 22.2 ± 0.08%, lignin 26.3 ± 0.09%, ash 0.03 ± 0.001%, moisture 3.5 ± 0.05%. During the pre-treatment process, the reaction flasks were incubated in a shaker at 90 °C for 14 h [29].

2.3.2. Dark fermentation

Please refer to Supplementary materials – Section S.1.

2.3.3. Extraction process

The extraction of FF and HMF was performed by mixing 15 mL of C:DOL (1:2 molar ratio) with 10 mL of hydrolysates in a 50–mL beaker. The pH of hydrolysates was adjusted to 7. The mixture was stirred for 50 min at 700 rpm at 40 °C. The concentration of FF and HMF was determined using headspace analysis coupled to gas chromatography with flame ionization detector (HS-GC-FID). In the studies, headspace analysis was used to avoid direct injecting of "dirty" aqueous hydrolysates into the GC system. The hydrolysates contain many non-volatile components (i.e. sugars, inorganic salts, polyphenols) that can cause contamination of a GC injector and a column thus shortening the stationary phase lifespan. The use of the HS technique allows the introduction of gas phase containing only volatile components into the injector. Theoretically, it is possible to perform similar DES phase analysis. However, some DES components, i.e. decanoic acid, are characterized by partial volatility and boiling point similar to HMF. Therefore, injecting the DES phase enriched with HMF and FF after incubation would cause co-elution of the chromatographic peaks, which would preclude correct studies. On the other hand, direct injecting of DES containing only partly volatile components would also contaminate the GC system. Therefore, in these studies only the headspace of aqueous hydrolysates was analyzed by GC-FID.

After the extraction process, 2 mL of water hydrolysates were transferred to the 20-mL vials and incubated for 40 min at 80 °C. After the incubation, 0.5 mL of the gas phase was analyzed with GC-FID.

The extraction efficiency (EE) was determined using the Eq. (1):

$$EE[\%] = \frac{C_{IN} - C_{Fin}}{C_{IN}} \cdot 100\% \quad (1)$$

where: C_{IN} – initial concentration of FF and HMF in hydrolysates [g/L], C_{Fin} – final concentration of FF and HMF in hydrolysates [mg/L].

The partition coefficients (K) were determined using the Eq. (2):

$$K = \frac{C_{DES}}{C_{hyd}} \quad (2)$$

where: C_{DES} – concentration of FF and HMF in the DES phase, C_{hyd} – concentration of FF and HMF in the hydrolysates after extraction.

2.3.4. Chromatographic analysis

Please refer to Supplementary materials–Section S.2.1.

2.3.5. Spectroscopic analysis and physicochemical properties of DES

Please refer to Supplementary materials–Section S.2.2.

2.3.6. Theoretical studies

Please refer to Supplementary materials–Section S.2.3.

3. Results and discussion

3.1. Physicochemical properties of DESs

In order to use DESs as extraction solvents, they must be liquid at the extraction temperature. Most of the individual components used for the DESs synthesis are solids at room temperature and their melting points are 179.8, 31.5 and 45 °C for C, DecAc and Xyl, respectively. Only DOL is liquid at ambient temperature (MP = 6.4 °C). Melting point of the synthesized DESs are 1, 19 and −45 °C for C:DOL, C:DecAc, and C:Xyl, respectively.

Most of DESs exhibit relatively high viscosities (>100 mPas) at room temperature [19]. However, dynamic viscosity of DESs should be as low as possible to ensure fast extraction kinetics. The values of viscosity at room temperature (25 °C) are 12.1, 10.7 and 18.9 mPas for C:DOL, C:DecAc and C:Xyl respectively. The viscosity of DESs decrease with an increase of temperature in all cases, which indicate normal liquid behavior. The deviations in dynamic viscosity are a function of the intermolecular interaction of the size and shape of the molecules. Increase in temperature diminishes the intermolecular interactions between components because of the increase in the thermal energy, which leads to less negative values of dynamic viscosity [30].

Usually, DESs have densities in the range of 1.0–1.35 g/cm^3 at 25 °C and atmospheric pressure or higher if they contain metallic salts in the structure, such as $ZnCl_2$ [19]. The densities of DESs composed of C and DecAC and DOL in 1:2 molar ratio are lower than water (0.85 and 0.87 g/cm^3). Only C:Xyl density is higher than water (1.09 g/cm^3). To accelerate the separations of DESs and aqueous phase after the extraction process, the difference of the density between the DES and water should be as large as possible. The largest density difference relative to water is revealed by C:DecAc. The C:DOL shows a slightly lower viscosity difference at room temperature. For all studied DESs, densities values were found to decrease linearly with the increase in temperature resulting from thermal expansion of the liquid. This is due to the fact that with increasing temperature the strength of the hydrogen bond weakens and thereby decreases the molecular distance [31]. The effects of temperature on dynamic viscosity and density of the studied DESs are shown in Fig. 1.

In order to ensure high EE of FF and HMF from aqueous samples, the water solubility in DESs should be as low as possible. The water solubility were 74.5 mg/L, 57.9 mg/L, and 3208.2 mg/L in C:DecAc, and C:DOL, C:Xyl, respectively. The C:DOL and C:DecAc were characterized by similar hydrophobicity, while most water dissolved in C:Xyl, which can significantly reduce the efficiency of FF and HMF extraction.

3.2. Structures and mechanism of DESs formation

In order to experimentally elucidate the structures of the new DESs formed, ^{1}H NMR and ^{13}C NMR spectra were taken (Figs. S1–S3). All peaks in ^{1}H NMR and ^{13}C NMR spectra can be assigned to the HBA and HBD compounds. No additional peaks are observed on the spectra, as indicated the occurrence of side reactions are observed.

For determination of the interaction between HBA and HBD in DESs, the proton chemical shifts (δδ) were described. The results of the differences between the chemical shift of the H proton of the OH group with respect to pure DOL and H proton of the OH group with respect to C:DOL indicate that the chemical shift value of the H proton of the OH group in C:DOL (δδ H-DOL = 1.84 ppm) as compared to the chemical shift of the H proton of the OH group in DOL (δδ H-C:DOL = 1.79 ppm) is reduced by 0.05 ppm (Fig. S1). This indicates the formation of a hydrogen bond between the -OH group in DOL and the C molecule. Similar results were also obtained in C:DecAc and C:Xyl, for which the positive H proton shifts of the -OH and -COOH group were 0.30 ppm and 0.21 ppm, respectively (Figs. S2, S3).

The interactions between HBA and HBDs resulting in formation of DES, were also investigated by FT-IR analysis (Figs. S4–S6). On all DESs spectra, the bands which can be attributed to the -OH group stretching vibration (3800–3100 cm^{-1}) and the C═O group stretching vibration (1600–1700 cm^{-1}) are observed. In the spectra of C:DOL and C:Xyl, a shift of the -O-H group band for a pure HBDs towards higher wavenumber values is observed. This indicates the formation of hydrogen bonds between HBA and HBDs. Similar behavior was also observed in the previous studies [20]. In the spectrum of C:DecAc, the peaks of -OH group, and the C═O group are shifted towards lower wavenumber values, this may be due to the gradual distribution of the –COOH group, which is caused by the formation of hydrogen bond in DES. Furthermore, the formation of all DESs can be confirmed by additional peaks present on the DESs spectra in the range of 500–1500 cm^{-1}.

Peak shifts on the FT-IR spectra are not unambiguous and they only provide information on the presence of strong hydrogen bonds between HBA and HBD. Therefore, theoretical studies based on quantum mechanics calculations were carried out for better understanding of the mechanism of DES formation. The most stable gas phase configurations of DESs were separately optimized at the B3LYP/6-311++G** level of theory (Fig. 2). All structures indicate the existence of non-bonded interactions between C and HBDs, which can be identified as strong hydrogen bonds because of the short distances between atoms (below 2.5 Å). The distances between the oxygen atom in the HBA and the hydroxyl groups in HBDs ═O···HO are 1.91 Å, 2.17 Å and 1.96 Å, 1.88 Å in C:DOL and C:Xyl respectively. In C:DecAc the distances of ═O···HOOC are 1.82 Å and 1.96 Å.

Electrostatic potential (ESP) analysis was used to qualitatively understand the configurations of new DESs. ESP isosurface plots provide a visualization of the total charge distribution and relative polarity of the studied DES structures. The ESP of DESs are mapped onto their

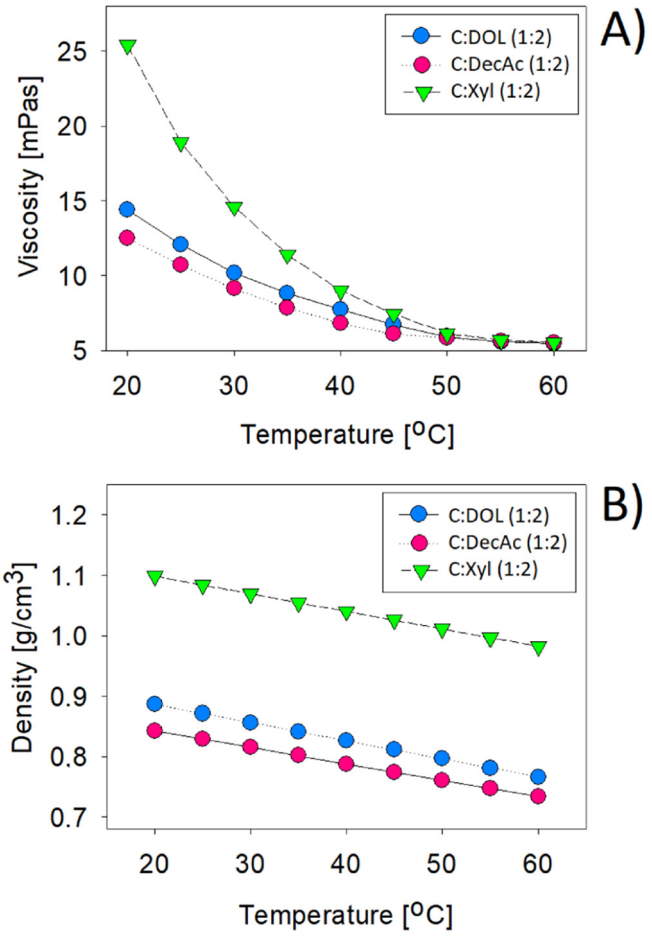

Fig. 1. A) Viscosities for DESs as a function of temperature, B) Densities for DESs as a function of temperature.

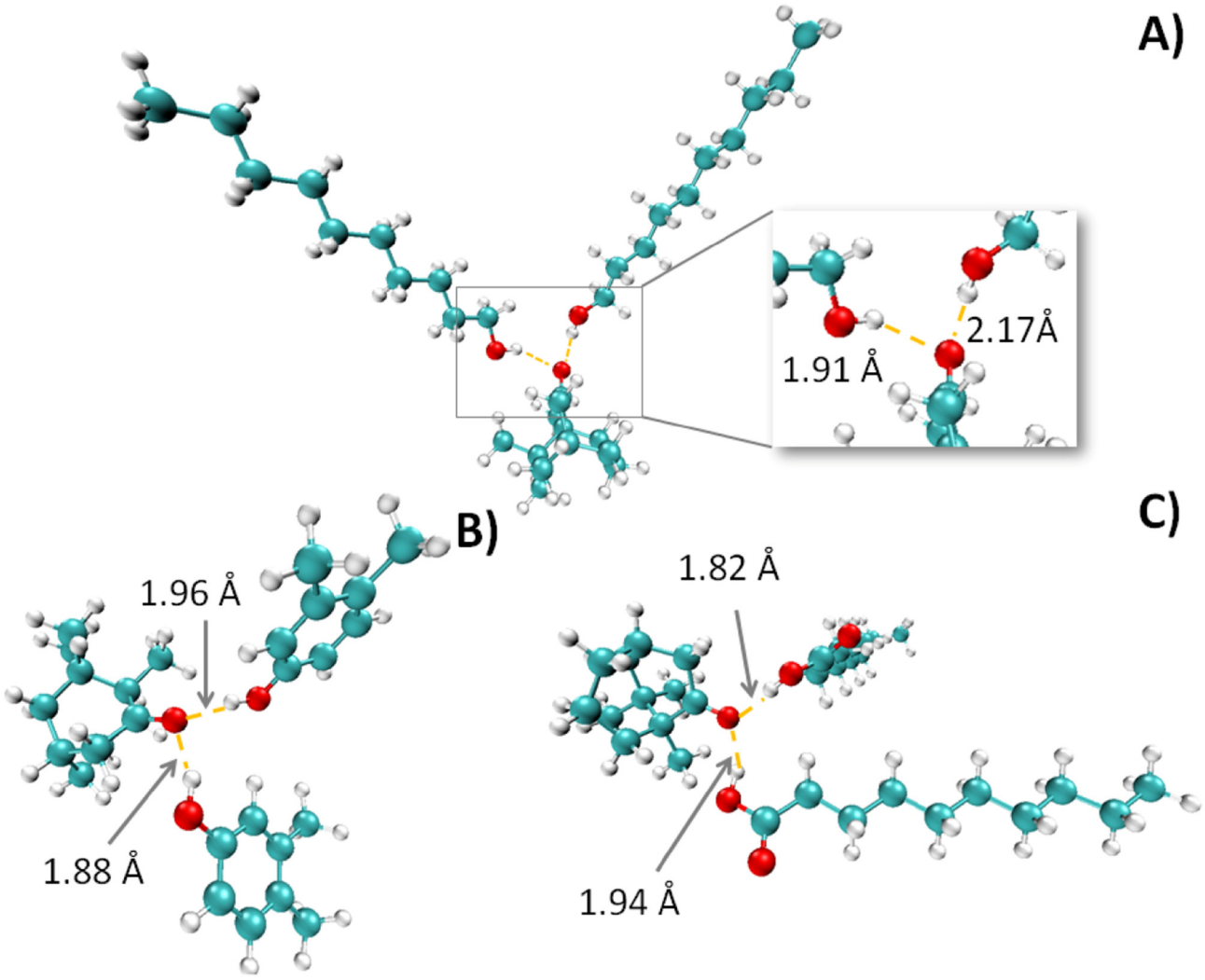

Fig. 2. Optimized structures of A) C:DOL, B) C:Xyl, C) C:DecAc.

electron densities in Fig. 3. The results demonstrate that the electronegative area is located around the O atom in C, whereas the electropositive area is around the rest part of C molecule. In DOL, Xyl and DecAC, the large electronegative areas are also located around the O atoms, whereas other positive areas are close to hydrogen atoms. Theoretically, during the formation of DES, the electronegative area of C should be close to the electropositive area of HBD (DOL, DecAc or Xyl). The stable DES configurations, which are presented in Fig. 3, confirm this prediction.

Reduced density gradient (RDG) was used as a tool for visualization of weak non-covalent interactions, by plotting the RDG versus the electron density multiplied by sign of the second Hessian eigenvalue [32]. In Fig. 4 the blue regions indicate strong attractive effects - hydrogen bond. The red regions denote strong repulsive interactions, for instance, ring, closure or steric effect, while green regions represent weaker interaction i.e. van der Waals interaction. Fig. 4 indicates that two hydrogen bonds were formed between HBA and HBDs in all tested DESs, which corresponds to large, negative sign of $(\lambda_2)\rho$ value (from −0.04 to −0.02 au) in 2D diagram (Fig. S5). In addition, Figs. 4 and S7 demonstrate that the van der Waals interactions occur in all DESs between HBA and HBDs, with values of 0.01 au < sign$(\lambda_2)\rho$ < 0.01 au. In DES composed of C and Xyl, strong repulsive bonds occur (sign$(\lambda_2)\rho$=0.02 au) due to the presence of an aromatic ring in the HBD structure. The coexistence of these types of interactions between HBA and HBD corresponds to the formation of stable DES structures, and to the decrease in melting points in DESs in comparison to the pure components.

3.3. Extraction conditions optimization

3.3.1. DES type

The type of solvent has a major effect on the FF and HMF removal from hydrolysates. In the studies, three DESs (C:DOL, C:Xyl, and C:DecAc) were tested, using the following pre-selected extraction conditions i.e. time of extraction 40 min, pH 7, extraction temperature 20 °C and 1:1 V_{DES}:V_{HYD} ratio. Fig. 5 demonstrates that C:Xyl had very low EE of FF and HMF as compared to the other solvents. This is probably due to the relatively high viscosity and high water solubility in C:Xyl. The highest EE for FF and HMF was obtained using C:DOL and slightly lower using C:DecAc. Thus, C:DOL was selected for further consideration. The obtained results indicate the relationship between hydrophobicity of DESs and EE. It can be observed that EE decreases along with an increase in hydrophobicity of DESs.

3.3.2. Response surface methodology

The most important parameters affecting EE were used to plan a subsequent higher order 2^2 design by means of central composite design (CCD). CCD consist of edge points (+1 and −1), which correspond to the upper and lower limits of the investigated factor, star points (−α

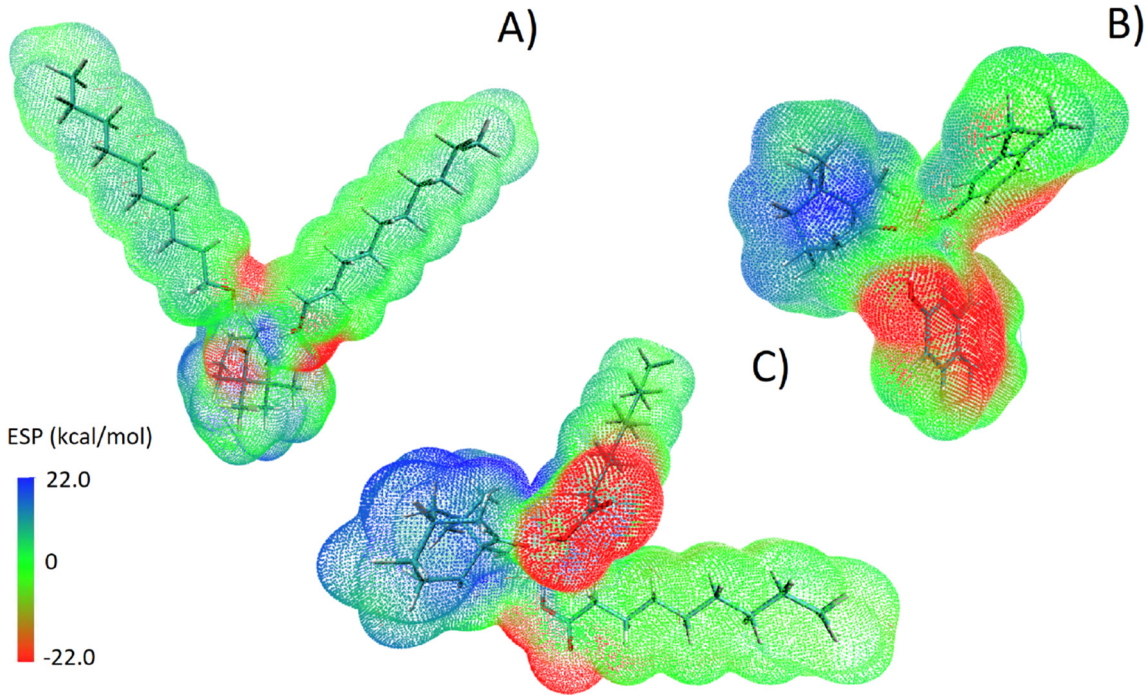

Fig. 3. Electrostatic potential mapped on electron total density with an isovalue 0.001 for A) C:DOL, B) C:Xyl, C) C:DecAc. Blue color-positive charges, red color–negative charges.

and +α), and zero levels. The value of α depends on the number of factors (k) and it is equal to $2^{k/4}$. According to the studies, four factors including V_{DES}:V_{HYD}, pH, extraction time and temperature were found to be significant for optimization. Table 1 demonstrates extended values for all the parameters in five levels and the design matrix and responses for the percentage of EE of FF and HMF from hydrolysates are given in Table S1.

To find the most important effects and interactions, analysis of variance (ANOVA) was calculated (Tables S2, S3). In ANOVA, the statistical F- and *p*-values were adopted as the criteria at a 95% confidence level. The *p*-value <0.05 indicates the statistically significant and influential factor on the statistic model. In the studies, the p-value of the models was found to be statistically significant due to the p-value <0.0001, and F-values equal to 55.2 and 83.9 for FF and HMF respectively. The *p*-values of lack of fit (p-value>0.088) relative to the pure error were considered insignificant.

The response equations obtained for the experimental results of FF and HMF can be expressed as follow:

$$Y_{FF} = -431.0 + 12.186\,X_1 + 23.67\,X_2 + 6.277\,X_3 + 106.9\,X_4 - 0.0995\,X_1 \times X_1 - 1.518\,X_2 \times X_2 - 0.06715\,X_3 \times X_3 - 38.41\,X_4 \times X_4 - 0.0968\,X_1 \times X_3 \quad (3)$$

$$Y_{HMF} = -505.8 + 17.12\,X_1 + 28.88\,X_2 + 6.51\,X_3 + 75.5\,X_4 - 0.1654\,X_1 \times X_1 - 1.887\,X_2 \times X_2 - 0.0903\,X_3 \times X_3 - 36.37\,X_4 \times X_4 - 0.0811\,X_1 \times X_3 \quad (4)$$

where Y_{FF} and Y_{HMF} are the EE of FF and HMF; X_1, X_2, X_3, X_4 are the independent variables. The models of FF and HMF presented a high determination coefficient (R^2 = 98.9 and 98.34% for FF and HMF, respectively), along with the values of predicted-R^2 (R^2_{pred} = 93.42 and 90.46%) and adjusted determination coefficient (R^2_{adj} = 97.72 and 96.56%). The obtained results indicate a good correlation between the experimental data, good fitting of the model and possibility of prediction of responses for new data.

The parameters i.e. time (X1), pH (X2), temperature (X3), and V_{DES}: V_{HYD} (X4) had significant linear effect on EE of FF and HMF. In addition, interactive effect of time and temperature (X1 * X3) was also significant (Tables S2, S3).

Time is one of the important parameters in any industrial process. Based on the observations, it can be concluded that the EE of FF and HMF increases along with the increase in extraction time, (Figs. 6, 7). This is probably due to the increased solubility of FF and HMF in C:DOL during mixing, which facilitates the mass transfer of FF and HMF from the hydrolysates to C:DOL phase. In addition, it can be observed that the extraction equilibrium was reached after 40 min and further extension of time did not improve the extraction yield.

The pH of hydrolysates is also a key parameter, which could affect EE. The results indicate that in the neutral pH 7 the structures of FF and HMF are suitable for extracting by C:DOL (Figs. 6, 7). Similar results were also obtained in the other studies [20,33]. Under basic conditions, compounds may have been ionized, especially HMF due to the -OH group in the structure, which caused reduced extraction efficiency. On the other hand, strong acidic conditions also resulted in a reduction in the efficiency of FF and HMF extraction. The ionized form of the compounds is more suitable when ionic DES is used as the extraction solvent, because then the extraction mechanism relies on ion exchange. Other intermolecular interactions have a dominant influence on the extraction process using non-ionic DES [34].

The effect of temperature on FF and HMF extraction from the hydrolysates was studied in range of 20–60 °C. The results indicate that EE increases slightly when increasing the temperature from 20 to 40 °C (Figs. 6, 7). Furthermore, an increase in temperature from 40 to 60 °C results in a decrease in extraction efficiency yield. This indicates that too low temperature is insufficient to ensure high extraction efficiency of FF and HMF. This is probably due to a significant decrease in the dynamic viscosity of DES from 14.9 mPas (20 °C) to 8.2 mPas (40 °C), which facilitated mass transfer from the hydrolysates to DES. On the other hand, too high temperature is also not favorable because the interactions between C:DOL and FF, HMF are based on an exothermic reaction, which could be described by Van't Hoff law. This law states that for an exothermic reaction heat is released, making the net enthalpy change negative, which has a direct impact of the partition coefficient value between C:DOL and FF, HMF [35]. In addition, sugars can degrade under the influence of higher temperature. Caramelization and

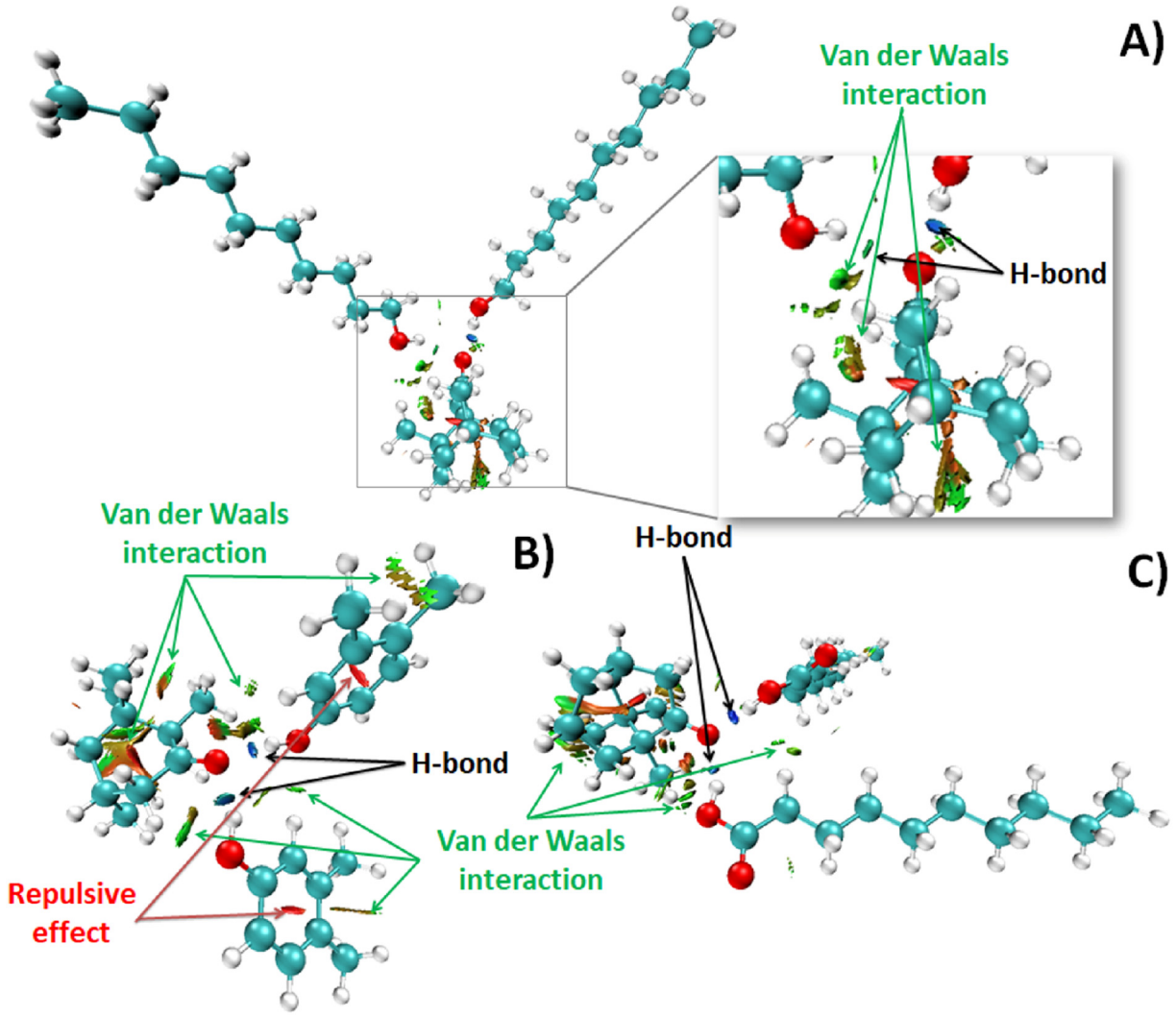

Fig. 4. RDG isosurfaces (s = 0.5 a.u.) of A) C:DOL, B) C:Xyl, C) C:DecAc.

subsequent pyrolysis of sugars may occur [36]. Consequently, this will reduce the efficiency of biogas production. Furthermore, the lower temperature is more favorable because of a lower energy consumption.

For most extraction processes, higher dosage of extraction solvent provides better EE. The results indicate that the maximum EE was obtained for V_{DES}:V_{Hyd} 1.5:1 (Figs. 6, 7). As the DES phase volume increased, the number of –OH active groups increased, which has a decisive impact on the extraction process efficiency. Further increase in the DES volume did not cause an increase in EE, which is advantageous from an economic point of view.

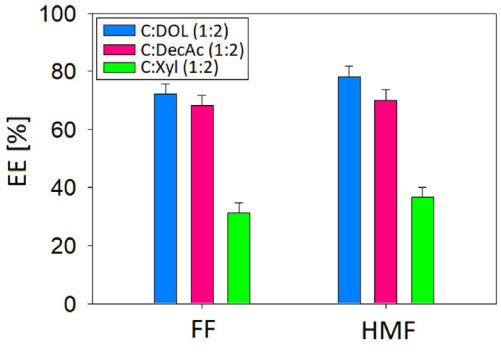

Fig. 5. The effect of type of DES on EE.

3.4. Mechanism of extraction

The studies on extraction mechanism were performed employing FT-IR analysis. In the spectrum of C:DOL, after the extraction process, the band corresponding to the -OH group increases its intensity and shifts towards lower wavenumber values (from 3867.00 cm^{-1} to 3845.66 cm^{-1} for HMF, and from 3867.00 cm^{-1} to 3844.95 cm^{-1} for FF) (Fig. 8). This indicates the formation of hydrogen bonds between C:DOL and FF and HMF, which determines the effective removal of fermentation inhibitors from the hydrolysates. In addition, all characteristic bands that can be assigned to HMF (3438.12–3111.16 cm^{-1}, 1252.44–1029.09 cm^{-1}, 733.99 cm^{-1}), and FF (3433.84–3118.78 cm^{-1}, 1263.16–1022.05 cm^{-1}, and 744.39 cm^{-1}) are visible in the DES spectrum after the extraction process. Similar results were also obtained for C:DecAc and C:Xyl (Fig. S8).

For better insight into the mechanism of FF and HMF extraction, the quantum mechanical analysis was also used. The results indicate that non-bonded interaction exists between all DESs and the fermentation inhibitors (Figs. 9 and S9). In the optimized configurations of C:DOL-FF, C:Xyl-FF and C:DecAc-FF, the distances between the oxygen atom

Table 1
Experimental ranges and levels of two variables in CCD.

Variables	Coded name	Ranges and levels (star points = $(2^k)^{1/4} = 2)^1$				
		−α	−1	0	+1	+α
Time of extraction [min]	X_1	10	20	30	40	50
pH	X_2	1	4	7	10	13
Temperature [°C]	X_3	20	30	40	50	60
V_{DES}:V_{HYD}	X_4	0.5:1	1:1	1.5:1	2:1	2.5:1

in the FF and hydroxyl group =O···HO or carboxylic group =O···HOOC of one of the HBD molecules are 2.01 Å, 2.30 Å, and 1.76 Å, respectively. This confirms the formation of a hydrogen bond between FF and one of the HBD molecules. Based on the distances, it can be concluded that between the oxygen atom in FF and -OH or -COOH group of the second HBD molecule there are weak electrostatic bonds. The optimized configuration of C:DOL-HMF indicates that two hydrogen bonds coexist between –OH group of FF and –OH groups of two DOL molecules (1.70 Å and 1.80 Å). In turn, in C:Xyl-HMF and C:DecAc-HMF complex, the hydrogen bonds are formed between –OH group of HMF and the oxygen atom in C molecule (1.90 Å and 1.82 Å) and between –OH group of HMF and –OH or -COOH group of one of the HBD molecules (1.82 and 1.78 Å). Additionally, based on the extension of the bonds length, it can be observed that when the FF and HMF molecules are attached to DESs, one of the hydrogen bonds between HBA and HBD in the DES structures becomes weaker.

The results of ESP analysis of the fermentation inhibitors demonstrate that the large electronegative areas are located around the O atom in FF and HMF, whereas other positive areas are close to hydrogen atoms (Fig. 10). When FF molecule interacts with C:DOL, the electronegative region located around O is attracted to the electropositive region located around the H atom in –OH group, forming hydrogen bond interaction. Whereas, the electropositive region of HMF located around the hydrogen atom in the -OH group attaches to the electronegative area located around oxygen in the DOL. In addition, the electronegative HMF region located around the oxygen atom in the -OH group attaches to the electropositive area located around oxygen in the -OH group of the second DOL molecule, which leads to the formation of two hydrogen bonds between HBD and HMF (Fig. 10). Similar results were also observed for other DES (Fig. S10).

The results of RDG analysis indicate that hydrogen bonds as well as van der Waals interactions occur in the C:DOL-FF, C:DOL-HMF, C:Xyl-FF, C:Xyl-HMF, C:DecAc-FF, and C:DecAc-HMF complexes (Figs. 11 and S11, S12). Two hydrogen bonds can be identified in the DES-FF complexes, one between HBA and HBD and the other between FF and HBD, as well as van der Waals interactions between FF, HBA and HBD. Whereas, in the DES-HMF complexes three hydrogen bonds as well as numerous van der Waals interactions can be identified between HMF, HBA and HBDs.

The interaction energy between DES and FF/HMF is generally negative. More negative values indicate stronger interactions inside a complex. The interaction energies between DES and the fermentation inhibitors are present in Table 2. The interaction energy followed a similar trend to that of the experimental EE of FF and HMF (C:DOL<C:DecAc<C:Xyl).

3.5. Reusability and regeneration of DES

Capability of reusing and recycling of an extraction solvent is one of its major benefits. Therefore, the reusability of C:DOL was examined. The results indicate that C:DOL becomes saturated and reduces its ability of FF and HMF extraction after 5 cycles. The extraction efficiency after 5 cycles decreased from 79.2 and 87.9% (K = 3.92 and 7.26) to 50.6 and 51.4% (K = 1.02 and 1.06) for FF and HMF, respectively (Fig. S13).

The regeneration and recycling of C:DOL were performed using adsorption process with activated carbon. The saturated C:DOL was shaken with activated carbon for 30 min at 25 °C, then centrifuged for 5 min at 7000 rpm and filtered through a 0.45 μm cellulose filter. After regeneration, C:DOL was recycled. The results indicate that slightly lower EE were obtained using recycled C:DOL (72.4% and 81.2% for FF and HMF respectively) than when using fresh C:DOL (79.2% and 87.9%). This is due to the fact that not all FF and HMF have been adsorbed on activated carbon. However, the efficiency of one-stage extraction using recycled DES is still high. As shown in Fig. S14, C:DOL can be recycled 12 times without noticeable decrease in EE.

3.6. Multistage extraction

The multistage extraction process can be used to achieve high EE. In the studies, EE at one step of extraction was 79.2 and 87.9% (K = 3.92 and 7.26) for FF and HMF, respectively. After each subsequent

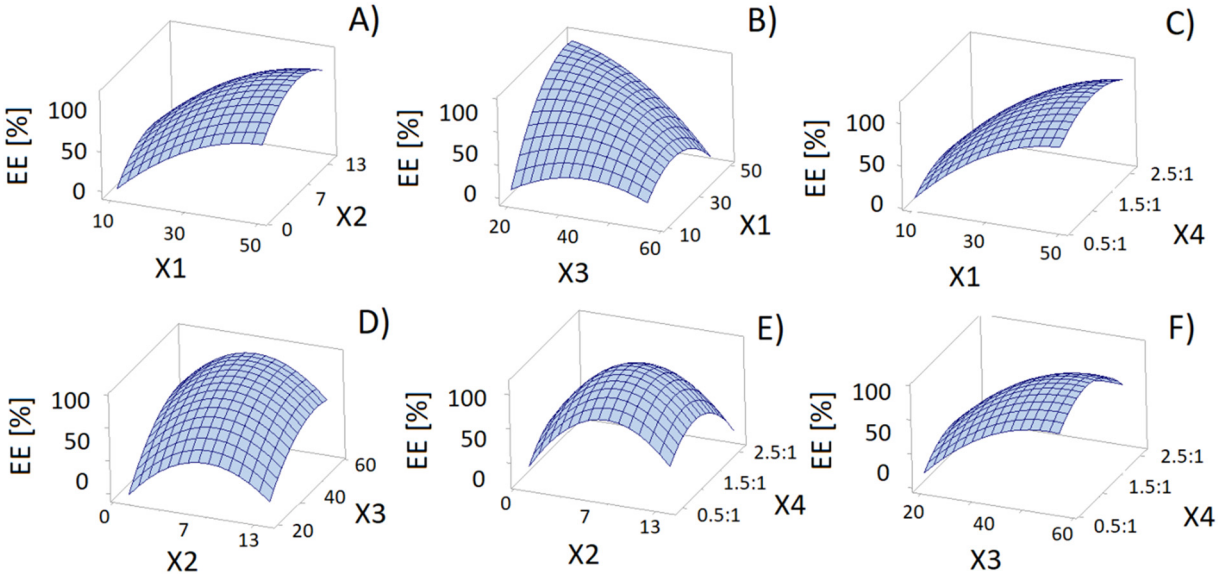

Fig. 6. Response surface plots for FF surface area dependence on: A) extraction time and pH, B) extraction time and extraction temperature, C) extraction time and V_{DES}:V_{HYD} ratio, D) pH and extraction temperature, E) pH and V_{DES}:V_{HYD} ratio, F) extraction temperature and V_{DES}:V_{HYD} ratio.

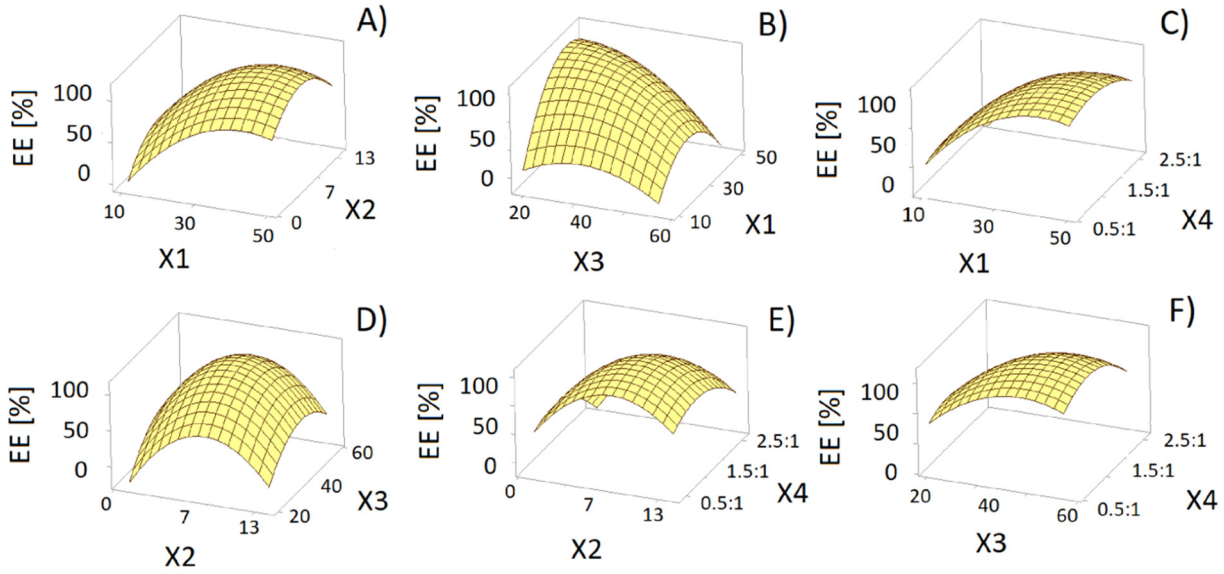

Fig. 7. Response surface plots for HMF surface area dependence on: A) extraction time and pH, B) extraction time and extraction temperature, C) extraction time and V_{DES}:V_{HYD} ratio, D) pH and extraction temperature, E) pH and V_{DES}:V_{HYD} ratio, F) extraction temperature and V_{DES}:V_{HYD} ratio.

extraction, the effectiveness of removing inhibitors increased. After four steps, the removal of FF and HMF reaches up to 99.99% (Fig. S15).

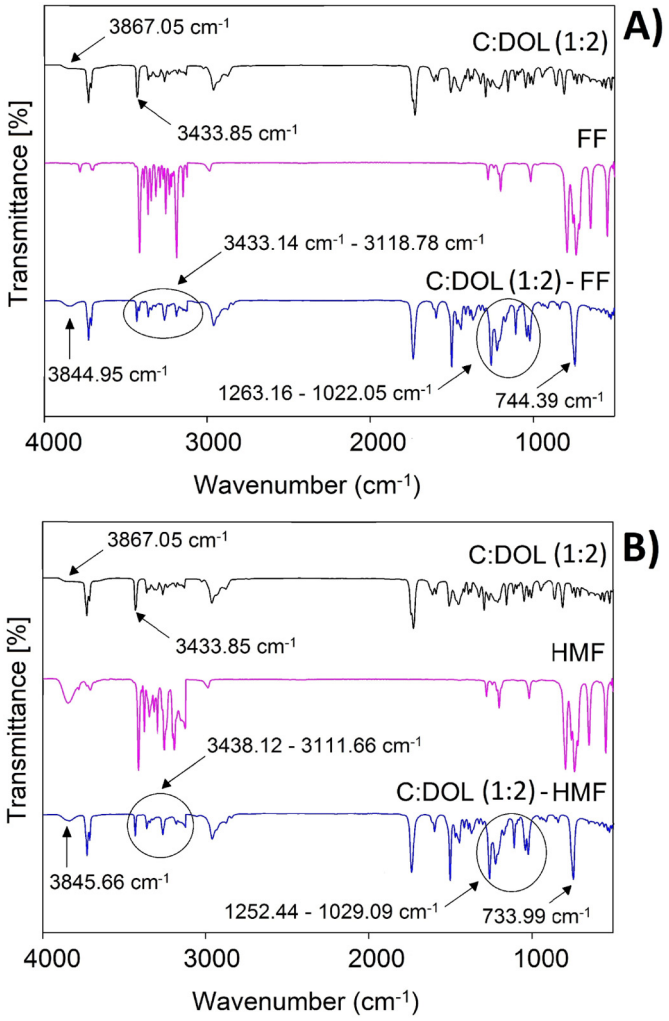

Fig. 8. FT-IR spectra of A) C:DOL, FF, and C:DOL-FF, B) C:DOL, HMF, and C:DOL-HMF.

3.7. Initial concentration of FF and HMF

The FF and HMF concentrations in the hydrolysates strongly depend on the type of raw material composition and conditions employed for hydrolysis. Typically, the concentrations range from 0.007 to 0.86 g/L and from 0.001 to 5.0 g/L, respectively for FF and HMF [12,37]. Therefore, in the studies the concentrations of FF and HMF in range from 0.01 to 5.0 g/L were examined. The results indicate that the initial concentration of FF and HMF slightly influences the EE of the studied DES. The EE slightly increased as the concentration of FF and HMF increased as follows: 0.01 g/L < 0.5 g/L < 1.0 g/L < 5.0 g/L (Fig. S16). This is an important result since it means that C:DOL is versatile for a wide range of FF and HMF concentrations, making it attractive in future industrial applications.

3.8. Solubility of sugars in DES

Most suited DESs should possess a high solubility for FF and HMF and a low solubility for sugars. Therefore, the influence of sugars removal from the model hydrolysate was also investigated. The results indicate that the sugars are not removed from the hydrolysates. This means that the extraction is highly selective for FF and HMF over sugars (Table S4). Similar results were also obtained for other type of DES in the previous studies [15].

3.9. Real hydrolysates – extraction efficiency and bio-hydrogen production

The extraction was also carried out for real hydrolysates. For the samples of EW NaOH and EW MEA hydrolysates, the efficiency of one-step extraction was 76.13 and 82.26% (K = 3.19 and 4.64) and 74.21 and 81.79% (K = 2.88 and 4.49) for FF and HMF, respectively. In addition, the lack of change in sugar concentration demonstrates great utility of the developed DES for the detoxification of hydrolysates. Slightly lower EE of FF and HMF were probably caused by the content of other fermentation inhibitors, i.e. phenols and organic acids, in the hydrolysates. Due to the presence of the -OH or -COOH group in their structures, these compounds can also be attached to DES with a hydrogen bond or van der Waals interactions. The results of FF, HMF, and sugars concentrations in the real samples of hydrolysates are present in Table 3. The comparison of the developed LLE procedure based on C:DOL as extraction solvent with other literature method showed that the proposed

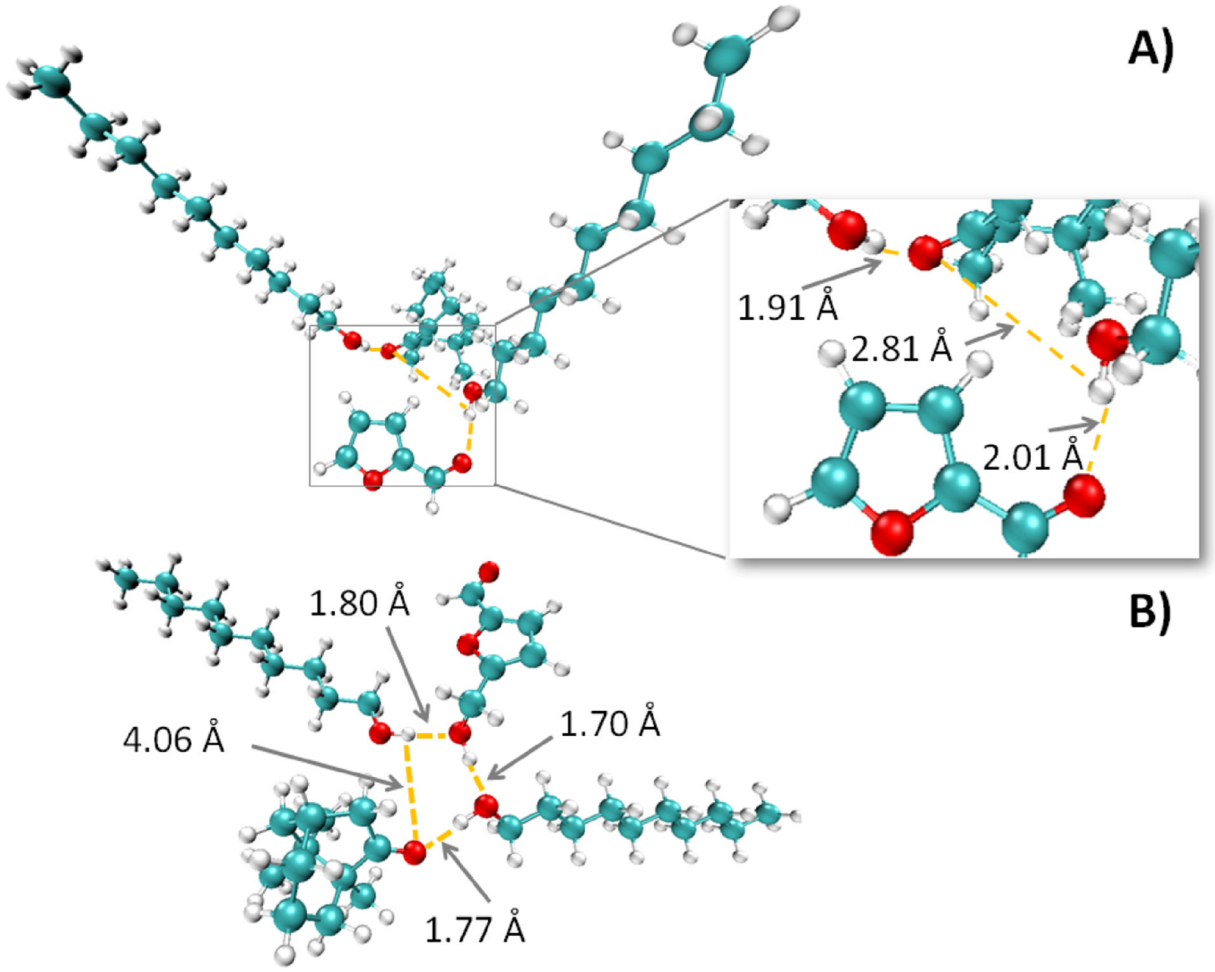

Fig. 9. Optimized configurations of A) C:DOL-FF, B) C:DOL-HMF.

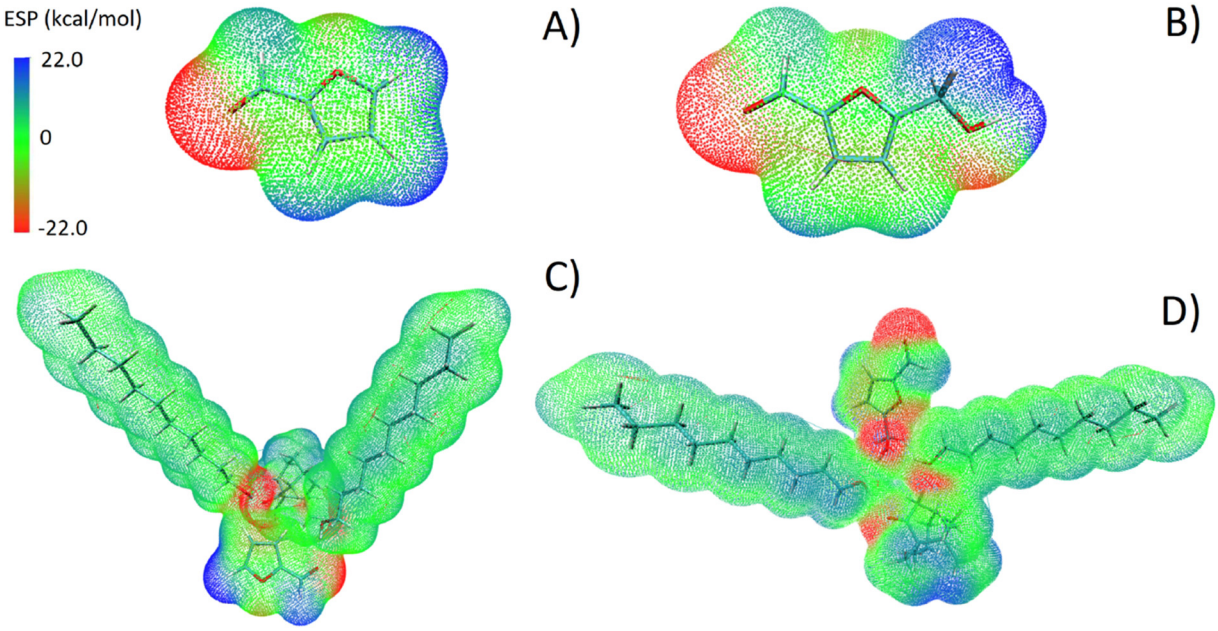

Fig. 10. Electrostatic potential mapped on electron total density with an isovalue 0.001 for A) FF, B) HMF, C) C:DOL-FF, D) C:DOL–HMF. Blue color represents positive charges, red color–negative charges.

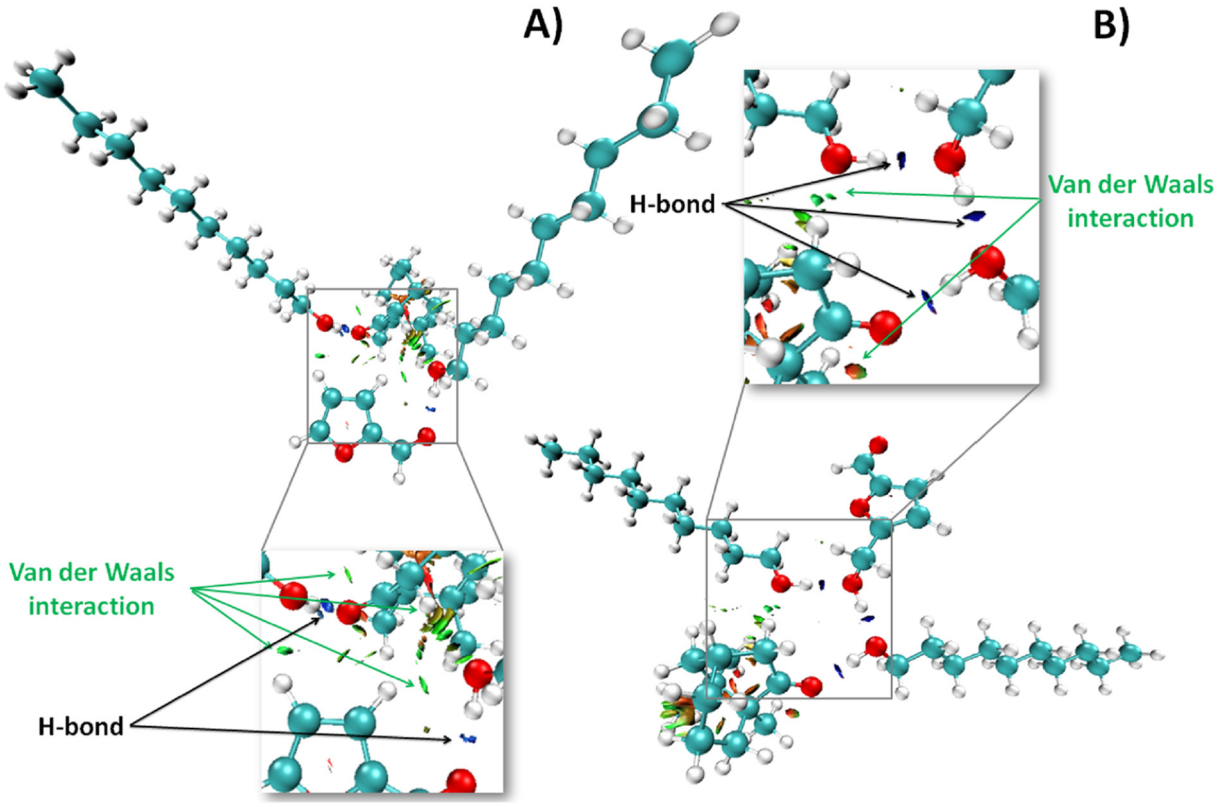

Fig. 11. RDG isosurfaces (s = 0.5 a.u.) of A) C:DOL-FF, B) C:DOL-HMF.

Table 2
Interaction energies between DES and fermentation inhibitors.

Complex	Interaction energy [kcal/mol]
C:DOL-FF	−12.51
C:DOL-HMF	−15.86
C:DecAc-FF	−11.60
C:DecAc-HMF	−12.56
C:Xyl-FF	−1.18
C:Xyl-HMF	−4.54

procedure had comparable EE in a single stage extraction (Table S5). However, the low price and green nature of C:DOL makes it a promising new solvent for removal of FF and HMF from hydrolysates.

In order to confirm the usefulness of the developed method, the purified hydrolysates were subjected to dark fermentation. The hydrogen production efficiency of 365 and 389 mL H_2/L total gas were obtained for EW NaOH and EW MEA, respectively. The results are comparable to those obtained using enzymatic hydrolysis in the previous studies [28,29]. However, as compared to the DES extraction, enzymatic hydrolysis is much more expensive, its duration can reach up to 1.5 days and requires large space and watchful control condition of microorganism growth.

4. Conclusions

A new hydrophobic DESs composed of non-toxic compounds were investigated for extractive detoxification of hydrolysates. The effect of some experimental variables on EE was studied, and it was concluded that the optimum extraction conditions were: extraction solvent C:DOL (1:2 molar ratio), extraction time 40 min, pH 7, temperature 40 °C, and V_{DES}:V_{Hyd} ratio 1.5:1. The EE of FF and HMF from the model hydrolysates was 79.2 and 87.9%, respectively after a single stage of extraction, which was further increased up to 99.99% after the fourth stage of extraction. After the extraction process, C:DOL was successfully regenerated and reused without loss of activity. The high EE of fermentation inhibitors from the real samples (higher than 74% and 82% for FF and HMF, respectively) without sugars loss, with low price, non-toxic nature, simple synthesis, and comparable bio-hydrogen yield to standard enzymatic hydrolysis procedure show tremendous application potential of C:DOL for detoxification of hydrolysates.

Table 3
Concentrations of FF, HMF, and sugars in real hydrolysates.

Compound	EW NaOH		EW MEA	
	Concentration before extraction [g/L]	Concentration after extraction [g/L]	Concentration before extraction [g/L]	Concentration after extraction [g/L]
FF	0.401 ± 0.018	0.0960 ± 0.0086	0.0101 ± 0.0014	$2.6 \cdot 10^{-3} \pm 3.1 \cdot 10^{-4}$
HMF	0.199 ± 0.012	0.0341 ± 0.0019	0.0212 ± 0.0023	$3.8 \cdot 10^{-3} \pm 3.8 \cdot 10^{-4}$
Cellobiose	0.402 ± 0.024	0.402 ± 0.022	1.37 ± 0.11	1.37 ± 0.10
Glucose	14.70 ± 0.89	14.65 ± 0.21	20.6 ± 0.34	20.5 ± 0.38
Xylose	0.716 ± 0.048	0.716 ± 0.052	0.97 ± 0.066	0.97 ± 0.067
Galactose	0.782 ± 0.055	0.782 ± 0.061	0.78 ± 0.018	0.77 ± 0.029
Mannose and arabinose	0.851 ± 0.068	0.841 ± 0.065	1.36 ± 0.12	1.35 ± 0.11

The experimental and theoretical studies indicate that coexistence of hydrogen bonds and van der Waals interaction between HBA and HBD contributes to formation of stable DES structures and to the decrease in the melting points of DES as compared to the pure components. Furthermore, the same interactions are the main driving forces for the removal of FF and HMF from hydrolysates.

CRediT authorship contribution statement

Patrycja Makoś: Writing - original draft, Conceptualization, Data curation, Methodology, Software, Investigation, Validation. **Edyta Słupek:** Writing - original draft, Investigation, Data curation, Methodology, Software. **Jacek Gębicki:** Supervision, Writing - review & editing.

Declaration of competing interest

The authors declare that they have no known competing financial interests or personal relationships that could have appeared to influence the work reported in this paper.

Acknowledgements

This research did not receive any specific grant from funding agencies in the public, commercial, or not-for-profit sectors.

Appendix A. Supplementary data

Supplementary data to this article can be found online at https://doi.org/10.1016/j.molliq.2020.113101.

References

[1] M. Raud, T. Kikas, O. Sippula, N.J. Shurpali, Potentials and challenges in lignocellulosic biofuel production technology, Renew. Sust. Energ. Rev. 111 (2019) 44–56, https://doi.org/10.1016/j.rser.2019.05.020.
[2] E. Słupek, P. Makoś, K. Kucharska, J. Gębicki, Mesophilic and thermophilic dark fermentation course analysis using sensor matrices and chromatographic techniques, Chem. Pap. (2019) https://doi.org/10.1007/s11696-019-01010-6*in press*.
[3] K. Kucharska, I. Hołowacz, D. Konopacka-Łyskawa, P. Rybarczyk, M. Kamiński, Key issues in modeling and optimization of lignocellulosic biomass fermentative conversion to gaseous biofuels, Renew. Energy 129 (2018) 384–408, https://doi.org/10.1016/j.renene.2018.06.018.
[4] P. Zhu, O.Y. Abdelaziz, C.P. Hulteberg, A. Riisager, New synthetic approaches to biofuels from lignocellulosic biomass, Curr. Opin. Green Sustain. Chem. 21 (2020) 16–21, https://doi.org/10.1016/j.cogsc.2019.08.005.
[5] B. Kumar, N. Bhardwaj, K. Agrawal, V. Chaturvedi, P. Verma, Current perspective on pretreatment technologies using lignocellulosic biomass : an emerging biore fi nery concept, 199 (2020) 106244–106268, https://doi.org/10.1016/j.fuproc.2019.106244.
[6] G. Kumar, P. Sivagurunathan, B. Sen, A. Mudhoo, G. Davila-Vazquez, G. Wang, S.H. Kim, Research and development perspectives of lignocellulose-based biohydrogen production, Int. Biodeterior. Biodegrad. 119 (2017) 225–238, https://doi.org/10.1016/j.ibiod.2016.10.030.
[7] C. Phuttaro, C. Sawatdeenarunat, K.C. Surendra, P. Boonsawang, S. Chaiprapat, S.K. Khanal, Anaerobic digestion of hydrothermally-pretreated lignocellulosic biomass: influence of pretreatment temperatures, inhibitors and soluble organics on methane yield, Bioresour. Technol. 284 (2019) 128–138, https://doi.org/10.1016/j.biortech.2019.03.114.
[8] D.L. Grzenia, D.J. Schell, S. Ranil Wickramsinghe, Detoxification of biomass hydrolysates by reactive membrane extraction, J. Memb. Sci. 348 (2010) 6–12, https://doi.org/10.1016/j.memsci.2009.10.035.
[9] D.L. Grzenia, D.J. Schell, S. Ranil Wickramasinghe, Membrane extraction for detoxification of biomass hydrolysates, Bioresour. Technol. 111 (2012) 248–254, https://doi.org/10.1016/j.biortech.2012.01.169.
[10] L. Pan, M. He, B. Wu, Y. Wang, G. Hu, K. Ma, Simultaneous concentration and detoxification of lignocellulosic hydrolysates by novel membrane filtration system for bioethanol production, J. Clean. Prod. 227 (2019) 1185–1194, https://doi.org/10.1016/j.jclepro.2019.04.239.
[11] T.R.K.C. Doddapaneni, R. Jain, R. Praveenkumar, J. Rintala, H. Romar, J. Konttinen, Adsorption of furfural from torrefaction condensate using torrefied biomass, Chem. Eng. J. 334 (2018) 558–568, https://doi.org/10.1016/j.cej.2017.10.053.
[12] G.B.M. Carvalho, S.I. Mussatto, E.J. Cândido, J.B. Almeida e Silva, Comparison of different procedures for the detoxification of eucalyptus hemicellulosic hydrolysate for use in fermentative processes, J. Chem. Technol. Biotechnol. 81 (2006) 152–157, https://doi.org/10.1002/jctb.1372.
[13] D. Ludwig, M. Amann, T. Hirth, S. Rupp, S. Zibek, Development and optimization of single and combined detoxification processes to improve the fermentability of lignocellulose hydrolyzates, Bioresour. Technol. 133 (2013) 455–461, https://doi.org/10.1016/j.biortech.2013.01.053.
[14] L.R. Roque, G.P. Morgado, V.M. Nascimento, J.L. Ienczak, S.C. Rabelo, Liquid-liquid extraction: a promising alternative for inhibitors removing of pentoses fermentation, Fuel 242 (2019) 775–787, https://doi.org/10.1016/j.fuel.2018.12.130.
[15] C.H.J.T. Dietz, F. Gallucci, M. Van Sint Annaland, C. Held, M.C. Kroon, 110th anniversary: distribution coefficients of furfural and 5-hydroxymethylfurfural in hydrophobic deep eutectic solvent + water systems: experiments and perturbed-chain statistical associating fluid theory predictions, Ind. Eng. Chem. Res. 58 (2019) 4240–4247, https://doi.org/10.1021/acs.iecr.8b06234.
[16] P. Cui, H. Liu, K. Xin, H. Yan, Q. Xia, Y. Huang, Q. Li, Liquid-liquid equilibria for the ternary system of water + furfural + solvents at 303.15 and 323.15 K under atmospheric pressure, J. Chem. Thermodyn. 127 (2018) 134–144, https://doi.org/10.1016/j.jct.2018.01.027.
[17] P. Makoś, G. Boczkaj, Deep eutectic solvents based highly efficient extractive desulfurization of fuels – eco-friendly approach, J. Mol. Liq. (2019) 111916–111927, https://doi.org/10.1016/j.molliq.2019.111916.
[18] D. Smink, S.R.A. Kersten, B. Schuur, Recovery of lignin from deep eutectic solvents by liquid-liquid extraction, Sep. Purif. Technol. 235 (2019) 116127–116133, https://doi.org/10.1016/j.seppur.2019.116127.
[19] P. Makoś, E. Słupek, J. Gębicki, Hydrophobic deep eutectic solvents in microextraction techniques–a review, Microchem. J. 152 (2020) 104384–104400, https://doi.org/10.1016/j.microc.2019.104384.
[20] P. Makoś, A. Przyjazny, G. Boczkaj, Hydrophobic deep eutectic solvents as "green" extraction media for polycyclic aromatic hydrocarbons in aqueous samples, J. Chromatogr. A 1570 (2018) 28–37, https://doi.org/10.1016/J.CHROMA.2018.07.070.
[21] P. Makoś, A. Fernandes, A. Przyjazny, G. Boczkaj, Sample preparation procedure using extraction and derivatization of carboxylic acids from aqueous samples by means of deep eutectic solvents for gas chromatographic-mass spectrometric analysis, J. Chromatogr. A 1555 (2018) 10–19, https://doi.org/10.1016/J.CHROMA.2018.04.054.
[22] C. Florindo, L.C. Branco, I.M. Marrucho, Development of hydrophobic deep eutectic solvents for extraction of pesticides from aqueous environments, Fluid Phase Equilib. 448 (2017) 135–142, https://doi.org/10.1016/J.FLUID.2017.04.002.
[23] L.F. Zubeir, D.J.G.P. Van Osch, M.A.A. Rocha, F. Banat, M.C. Kroon, Carbon dioxide solubilities in decanoic acid-based hydrophobic deep eutectic solvents, J. Chem. Eng. Data 63 (2018) 913–919, https://doi.org/10.1021/acs.jced.7b00534.
[24] E. Słupek, P. Makoś, J. Gębicki, Deodorization of model biogas by means of novel non- ionic deep eutectic solvent, Arch. Environ. Prot. 46 (2020) 41–46, https://doi.org/10.24425/aep.2020.132524.
[25] E. Słupek, P. Makoś, Absorptive desulfurization of model biogas stream using choline chloride-based deep eutectic solvents, Sustainability 12 (2020) 1619–1635, https://doi.org/10.3390/su12041619.
[26] C.L. Boldrini, N. Manfredi, F.M. Perna, V. Capriati, A. Abbotto, Designing ecosustainable dye-sensitized solar cells by the use of a menthol-based hydrophobic eutectic solvent as an effective electrolyte medium, Chem. - A Eur. J. 24 (2018) 17656–17659, https://doi.org/10.1002/chem.201803668.
[27] C.H.J.T. Dietz, M.C. Kroon, M. Van Sint Annaland, F. Gallucci, Thermophysical properties and solubility of different sugar-derived molecules in deep eutectic solvents, J. Chem. Eng. Data 62 (2017) 3633–3641, https://doi.org/10.1021/acs.jced.7b00184.
[28] R. Łukajtis, P. Rybarczyk, K. Kucharska, D. Konopacka-Łyskawa, E. Słupek, K. Wychodnik, M. Kamiński, Optimization of saccharification conditions of lignocellulosic biomass under alkaline pre-treatment and enzymatic hydrolysis, Energies (2018) 886–913, https://doi.org/10.3390/en11040886.
[29] K. Kucharska, R. Łukajtis, E. Słupek, H. Cieśliński, P. Rybarczyk, M. Kamiński, Hydrogen production from energy poplar preceded by MEA pre-treatment and enzymatic hydrolysis, Molecules 23 (2018) 3029–3050, https://doi.org/10.3390/molecules23113029.
[30] P.R. Naidu, V.R. Krishnan, Viscosities of binary liquid mixtures, Proc. Indian Acad. Sci. - Sect. A. 64 (1966) 229–236, https://doi.org/10.1007/BF03049393.
[31] N. Sudhir, P. Yadav, B.R. Nautiyal, R. Singh, H. Rastogi, H. Chauhan, Extractive desulfurization of fuel with methyltriphenyl phosphonium bromide- tetraethylene glycol-based eutectic solvents, Sep. Sci. Technol. (2019) 554–563, https://doi.org/10.1080/01496395.2019.1569061.
[32] E.R. Johnson, S. Keinan, P. Mori-Sánchez, J. Contreras-García, A.J. Cohen, W. Yang, Revealing noncovalent interactions, J. Am. Chem. Soc. 132 (2010) 6498–6506, https://doi.org/10.1021/ja100936w.
[33] M. Madani-Tonekaboni, M. Kamankesh, A. Mohammadi, Determination of furfural and hydroxymethyl furfural from baby formula using dispersive liquid-liquid microextraction coupled with high performance liquid chromatography and method optimization by response surface methodology, J. Food Compos. Anal. 40 (2015) 1–7, https://doi.org/10.1016/j.jfca.2014.12.004.
[34] C. Florindo, F. Lima, L.C. Branco, I.M. Marrucho, Hydrophobic deep eutectic solvents: a circular approach to purify water contaminated with ciprofloxacin, ACS Sustain. Chem. Eng. 7 (2019) 14739–14746, https://doi.org/10.1021/acssuschemeng.9b02658.
[35] K.H. Almashjary, M. Khalid, S. Dharaskar, P. Jagadish, R. Walvekar, T.C.S.M. Gupta, Optimisation of extractive desulfurization using choline chloride-based deep eutectic solvents, Fuel 234 (2018) 1388–1400, https://doi.org/10.1016/j.fuel.2018.08.005.
[36] I. Rykowska, J. Ziemblińska, I. Nowak, Modern approaches in dispersive liquid-liquid microextraction (DLLME) based on ionic liquids: a review, J. Mol. Liq. 259 (2018) 319–339, https://doi.org/10.1016/J.MOLLIQ.2018.03.043.
[37] B.G. Fonseca, R.D.O. Moutta, F.D.O. Ferraz, E.R. Vieira, A.S. Nogueira, B.F. Baratella, L.C. Rodrigues, H.R. Zhang, S.S. Da Silva, Biological detoxification of different hemicellulosic hydrolysates using Issatchenkia occidentalis CCTCC M 206097 yeast, J. Ind. Microbiol. Biotechnol. 38 (2011) 199–207, https://doi.org/10.1007/s10295-010-0845-z.